0012-9402/97/020229-16 $1.50 + 0.20/0
Birkhäuser Verlag, Basel, 1997

Eclogae geol. Helv. 90 (1997) 229–244

Integrated stratigraphy of the Tortonian/Messinian boundary: The Pietrasecca composite section (central Apennines, Italy)

Domenico Cosentino[1], Maria Gabriella Carboni[2], Paola Cipollari[1], Letizia Di Bella[2], Fabio Florindo[3], Marinella Ada Laurenzi[4] & Leonardo Sagnotti[3]

Key words: Biostratigraphy, magnetostratigraphy, geochronology, Tortonian/Messinian boundary, central Apennines

ABSTRACT

In the Pietrasecca section (central Apennines, Italy) the first occurrences (FOs) of *Globorotalia conomiozea* and *Amaurolithus delicatus*, which define the Tortonian/Messinian (T/M) boundary, were found in a reverse magnetozone (R2) together with the FO of *Amaurolithus primus*. Assuming that this bioevent was isochronous, as suggested by the correlation of the biochronology of the equatorial Pacific Ocean with that of the tropical Indian Ocean (Raffi et al. 1995), and taking into account the results from ODP Leg 138 (Eastern Equatorial Pacific), which show the FO of *Amaurolithus primus* within C3Br.2r (Raffi 1992; Raffi et al. 1995), it is possible to correlate the magnetozones recognised in the Pietrasecca section with Cande & Kent's (1992) Geomagnetic polarity time scale (GPTS) (CK92). Although in the Crete sections (Krijgsman et al. 1994) and in the northern Apennine sections (Vai, in press) the T/M boundary falls within chron C3Br.1r, the sedimentation rates calculated considering different magnetostratigraphic solutions show that for the Pietrasecca section the identification of R2 with C3Br.2r is the only realistic correlation to the CK92 GPTS.

In particular, the T/M boundary recognised in the Pietrasecca section occurs in the uppermost part of C3Br.2r. According to the CK92 GPTS its age is 7.0 Ma while the modified GPTS of Baksi (1993) provides an age of 7.1 Ma. These ages are slightly older than that calculated for the Crete section (6.92 Ma) by Krijgsman et al. (1994). Finally, using Cande & Kent's (1995) GPTS (CK95) as a reference, the age of the T/M boundary is 7.12 Ma for the Crete sections, as suggested by Krijgsman et al. (1995) considering the T/M boundary within chron C3Br.1r, and 7.18 Ma for the Pietrasecca section. In addition, the $^{40}Ar/^{39}Ar$ radiometric information obtained on plagioclase separated from a volcaniclastic level occurring at the T/M boundary (FO of *G. conomiozea*) in the Pietrasecca section (≤ 7.17 Ma) is in good agreement with the age of 7.15 ± 0.04 Ma obtained from a biotite sample at the T/M boundary at the Monte del Casino section in the Northern Apennines (Laurenzi et al., in press).

RIASSUNTO

Nella sezione di Pietrasecca (Appennino centrale), all'interno della porzione superiore delle Marne a Orbulina, è stata riconosciuta la prima comparsa sia di *Globorotalia conomiozea* che di *Amaurolithus delicatus*, che definiscono il limite T/M. La comparsa di queste specie si colloca in una magnetozona inversa (R2). All'interno della stessa magnetozona è stata riconosciuta, inoltre, la comparsa di *Amaurolithus primus*. Assumendo che questo bioevento sia isocrono, come suggerito dai risultati del settore equatoriale dell'Oceano Pacifico e della fascia tropicale dell'Oceano Indiano (Raffi 1992; Raffi et al. 1995) che pongono la FO (first occurrence) di *A. primus* all'interno del C3Br.2r, è possibile correlare le magnetozone riconosciute nella sezione di Pietrasecca con la GPTS (Geomagnetic polarity time scale) CK92 (Cande & Kent 1992). Inoltre i tassi di sedimentazione calcolati considerando diverse soluzioni magnetostratigrafiche mostrano che la identificazione della R2 con il C3Br.2r è l'unica correlazione realistica con la GPTS CK92, mentre, nelle sezioni di Creta (Krijgsman et al. 1994) e in quelle dell'Appennino settentrionale (Vai, in press) il limite T/M è riconosciuto all'interno del chron C3Br.1r.

In questo sistema di riferimento (CK92) il limite T/M riconosciuto nella sezione di Pietrasecca si colloca nella parte sommitale del C3Br.2r. Secondo la calibrazione della GPTS CK92 la sua età sarebbe di 7.0 Ma, mentre la GPTS modificata di Baksi (1993) fornisce un'età di 7.1 Ma. Queste età risultano leggermente più vecchie di quelle calcolate per la sezione di Creta (6.92 Ma) da Krijgsman et al. (1994), mentre sono in accordo con l'età di 7.12 Ma suggerita da Krijgsman et al. (1995) considerando il limite T/M posizionato all'interno del chron C3Br.1r e utilizzando la GPTS di Cande & Kent (1995) come riferimento. Inoltre, l'informazione radiometrica $^{40}Ar/^{39}Ar$ ottenuta su plagioclasio, separato dal livello vulcanoclastico che nella sezione di Pietrasecca si rinviene in corrispondenza del limite T/M (≤ 7.17 Ma) è in buon accordo con l'età di 7.15 ± 0.04 Ma ottenuta da un campione prelevato in corrispondenza del limite T/M nella sezione di Monte del Casino in Appennino settentrionale (Laurenzi et al., in press).

Introduction

This study is part of a broader research project concerning the definition of an integrated stratigraphy of the Neogene terrigenous deposits of the central Apennines, a necessary step to constrain the timing of the recent evolution of the Apenninic chain. In this paper we focus on the detailed magnetostratigraphy, biostratigraphy and radiometric dating of the Tortonian/Messinian (T/M) boundary, at the Pietrasecca composite section (central Apennines, Italy) (Fig. 1), and on the correla-

[1] Dip. Scienze Geologiche, Università degli Studi di Roma Tre, L.go S. Leonardo Murialdo 1, I–00146 Roma
[2] Dip. Scienze della Terra, Università degli Studi di Roma "La Sapienza", P. le A. Moro 5, I–00185 Roma
[3] Istituto Nazionale di Geofisica, Via di Vigna Murata 605, I–00143 Roma
[4] Istituto di Geocronologia e Geochimica isotopica, CNR, Via Cardinale Maffi 36, I–56127 Pisa

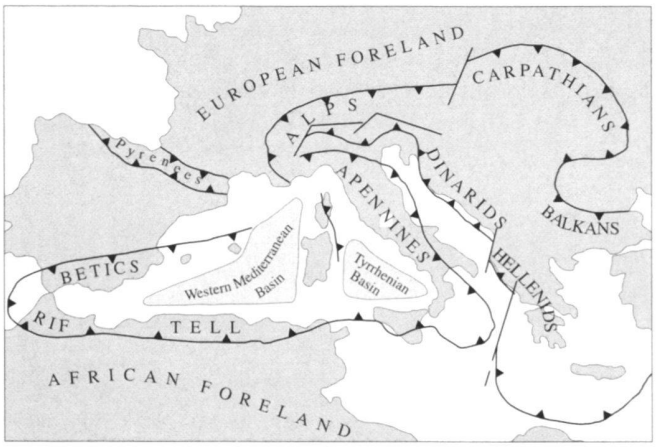

Fig. 1. Geological sketch of the Mediterranean area and location of the Pietrasecca section (white square).

tion of the identified magnetozones with Cande & Kent's (1992) geomagnetic reversal time scale (CK92). The Pietrasecca section is suitable for this study because of its peculiar characteristics of good exposure, fine grained lithology, apparently continuous sedimentation, and absence of tectonic disturbances. Moreover, a centimetric volcaniclastic level occurs within the upper Tortonian succession, providing the opportunity of obtaining a radiometric age.

Several attempts have been made, mainly in the Mediterranean region, to define this chronological boundary and in general to define a detailed Late Miocene chronostratigraphy, mainly by means of integrated magnetostratigraphic and biostratigraphic studies (Colalongo et al. 1979; Langereis et al. 1984; Moreau et al. 1985; Sierro 1985; Glacon et al. 1990; Benson & Rakic-El Bied 1991; Langereis & Dekkers 1992; Sierro et al. 1993; Vai et al. 1993; Cunningham et al. 1994; Hodell et al. 1994; Krijgsman et al. 1994; 1995; Hilgen et al. 1995; Laurenzi et al. in press; Negri & Vigliotti, in press; Vai, in press).

During the past decade, among others, Moreau et al. (1985), through a palaeomagnetic study of a Late Miocene section from the Moroccan Atlantic margin, found the First Appearance Datum (FAD) of *Globorotalia* gr. *conoidea conomiozea* and the FAD of *Amaurolithus* spp. in the normal polarity interval of the Chron 6n (Berggren et al. 1985) (correlated to the C3Bn magnetozone of CK92). The authors suspected either a remagnetization or a rapid change in the sedimentation rate in this portion of the section. This correlation is consistent with the results reported in a subsequent paper by Channel et al. (1990) in which, from a magnetostratigraphic investigation of sediments collected at ODP Site 654 in the Tyrrhenian Sea, the First Occurrence (FO) of *G. conomiozea* was found within a normal polarity interval, correlated to Chron 6n, implying an age of 6.4 Ma for the T/M boundary.

In 1992, Langereis & Dekkers investigated the paleomagnetism and the rock-magnetism of the T/M boundary stratotype at Falconara in southern Sicily. The results pointed out that the entire section was recently remagnetized (normal polarity remanent magnetizations of post-tilting age) and is therefore unsuitable to provide a direct time control on the biostratigraphic datum levels.

Vai et al. (1993) analysed five volcanogenic horizons interlayered within pre-evaporitic euxinic marls across the Tortonian/Messinian boundary in the outer units of the northern Apennine thrust belt (Monte del Casino and Monte Tondo sections). $^{40}Ar/^{39}Ar$ and K/Ar dating carried out on plagioclase and biotite selected from these volcanogenic horizons suggested an age of 7.26 ± 0.10 Ma for the Tortonian/Messinian boundary.

Krijgsman et al. (1994) discussed the age of the T/M boundary in some sections in the Crete island (Faneromeni, Kastelli and Skouloudhiana) previously studied by Langereis (1984) and Langereis et al. (1984). Using the planktic *G. conomiozea* First Occurrence Datum (FOD) as the T/M biostratigraphic marker, for this boundary they suggest an age ranging from 6.92 to 7.10 Ma depending on the reference geomagnetic polarity time scale.

Cunningham et al. (1994) published the results of a combined magnetostratigraphy, biostratigraphy and $^{40}Ar/^{39}Ar$ dating on a Tortonian-Messinian shallow-marine carbonate complex in northeastern Morocco. They found *G. conomiozea* in a reversed zone correlated, with reference to Benson & Rakic-El Bied (1991) and to the recently developed GPTS (Geomagnetic polarity time scale) of Shackleton et al. (in press), with the C3Ar subchron.

Krijgsman et al. (1995) suggested a new chronology for the Late Miocene of the Mediterranean, integrating magnetostratigraphic, biostratigraphic and cyclostratigraphic data. The Tortonian/Messinian boundary, defined by the First Regular Occurrence of the *G. conomiozea* group, is recognised in chron C3Br.1r with an age of 7.12 Ma according to the GPTS (CK95) of Cande & Kent (1995).

Laurenzi et al. (in press) provided new $^{40}Ar/^{39}Ar$ radiometric datings on biotites collected from a series of biotite-rich volcaniclastic horizons spanning the Tortonian/Messinian boundary in the Monte del Casino sections in the northern Apennines. These datings allow the T/M boundary to be bracketed in a range from about 7.08 to about 7.16 Ma.

Geological setting of the Pietrasecca area

The Pietrasecca section is located in the Carseolani Mts. (central Apennines), about 50 km NE of Rome (Fig. 1). The central Apennines are a post-collisional thrust belt developed in an ensialic context, mainly during Neogene time, as a consequence of the A-type subduction of the Adria microplate beneath the European plate (Boccaletti et al. 1971; 1980; Boccaletti & Guazzone 1972; Scandone 1979; Aubouin et al. 1980, Mantovani et al. 1985).

This area is characterised by pre-orogenic Meso-Cenozoic shallow-water carbonates, belonging to the Latium-Abruzzi

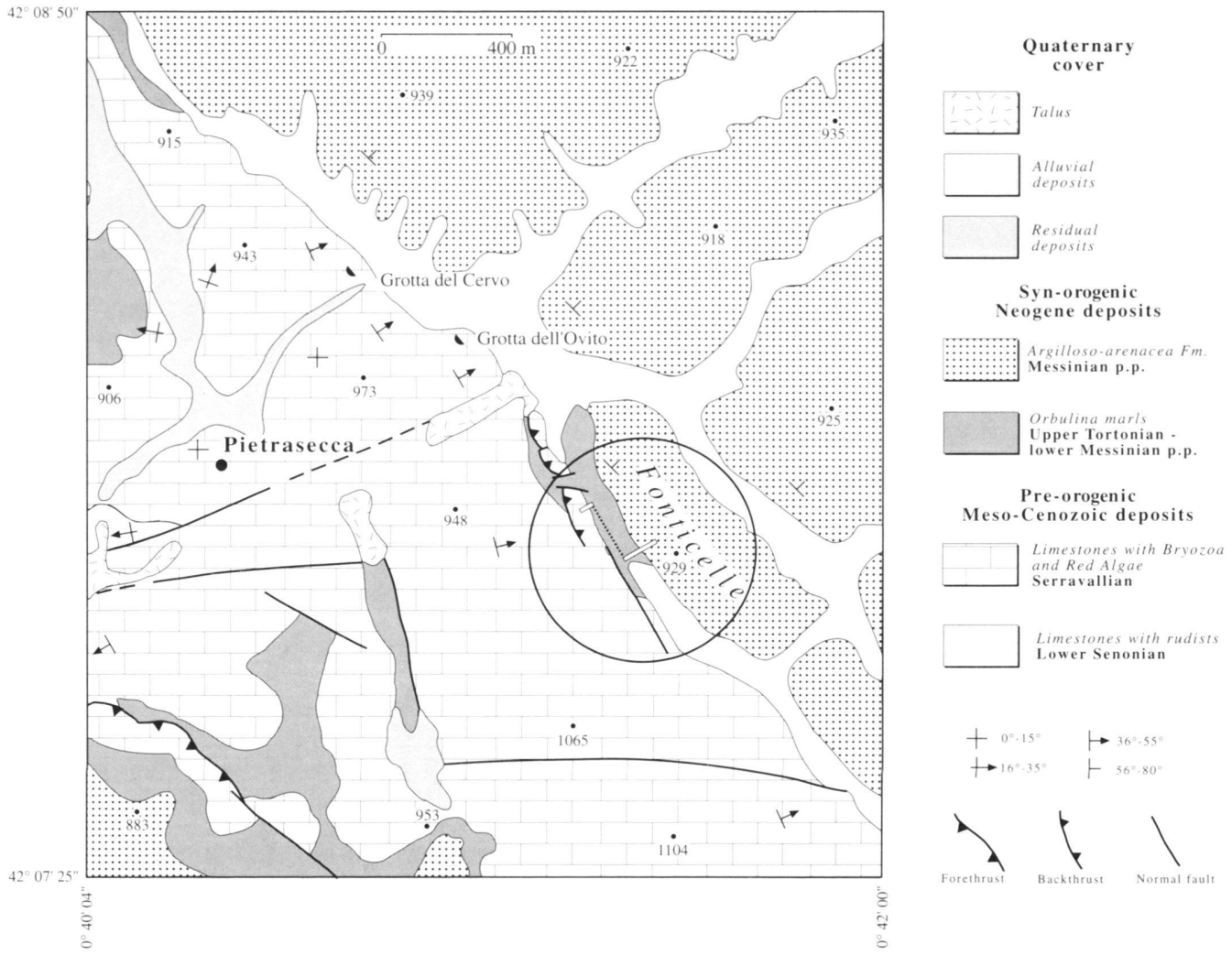

Fig. 2. Geological map of the Pietrasecca area (after Agostini 1993; modified). The circle indicates the location of the Pietrasecca section.

carbonate platform (Parotto & Praturlon 1975), which are overlain by Late Miocene syn-orogenic terrigenous deposits related to an Apennine foredeep basin (*Argilloso-arenacea* Fm., Cipollari et al. 1993).

During the Messinian *lago-mare*/Early Pliocene Apennine tectonic event (Patacca et al. 1992; Cipollari et al. 1995; Cipollari & Cosentino 1996), the area underwent a compressional tectonic phase and was involved in the accretion of the central Apennine tectonic wedge. This tectonic phase, which affected mainly the sedimentary cover, induced a shortening of about 50% generating folds and thrusts in the Meso-Cenozoic carbonate and terrigenous deposits.

From a structural point of view, the Pietrasecca area is characterised by a NE-vergent macro-anticline with a NW-plunging axis (Pietrasecca-Tufo anticline). The Pietrasecca section is located on the forelimb of the Pietrasecca-Tufo anticline (Fig. 2).

The Pietrasecca section

The section is located on the western flank of the Fonticelle rise, 1.5 km ESE from the Pietrasecca village. It is about 60 m-thick; the stratigraphic boundary between the *Calcari a briozoi e litotamni* Fm. and the overlying *Marne a Orbulina* Fm. is recognisable in its lower portion. This boundary marks the change from carbonatic to terrigenous sedimentation and represents the involvement of the Adria foreland in the Apennine chain-foredeep system (foreland flexure stage).

According to Compagnoni et al. (1992) and Pampaloni et al. (1994), three different lithofacies may be recognised in the

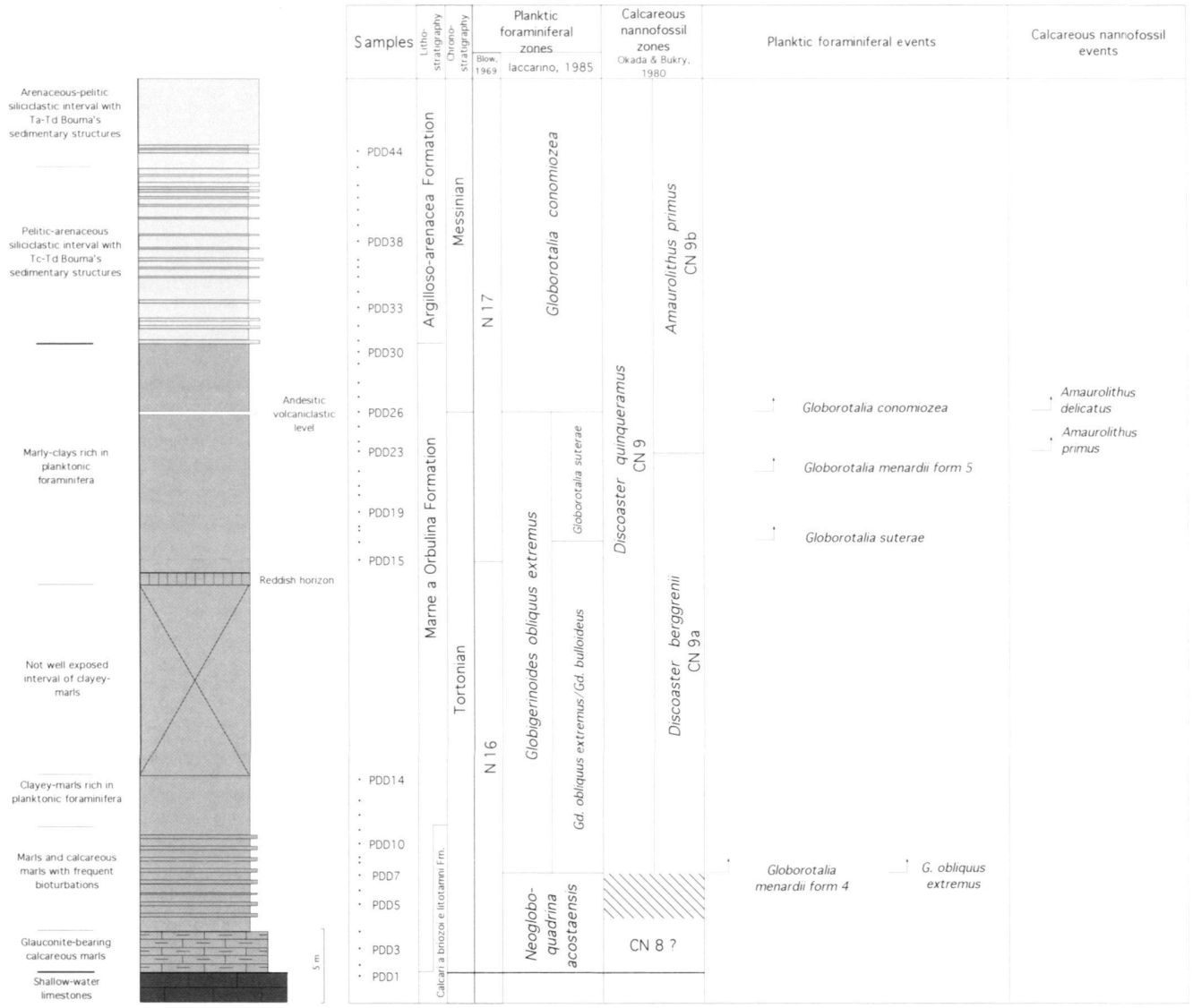

Fig. 3. Lithostratigraphy, chronostratigraphy, biochronology and bioevents of the Pietrasecca section.

Marne a Orbulina Fm. However, the results of our field work carried out in the Pietrasecca section (Fig. 3) are slightly different from those presented by Pampaloni et al. (1994). The lower part of the *Marne a Orbulina* Fm. is made up of 2.5 m of calcareous marls rich in glauconite nodules, with common shelly macrofossils, fish teeth, benthonic and rare planktonic foraminifera. This lower portion corresponds to lithofacies 1 of Pampaloni et al. (1994).

Upsection, these calcareous marls pass to a 7 m-thick, cyclic alternation of marls and calcareous marls rich in planktonic foraminifera, often bioturbated by fucoids and *Zoophycos*. This portion of the Pietrasecca section corresponds to lithofacies 2 of Pampaloni et al. (1994).

Above the cyclic alternation, the prevailing lithologies are clayey-marls, gradually passing to marly-clays rich in planktonic foraminifera (Fig. 4). This lithofacies characterises 75% of the total thickness (*i.e.* 30 m) of the *Marne a Orbulina* Fm. The middle-basal portion of this lithofacies, 10 out of 30 m, is not well exposed (Fig. 3). The middle portion is characterised by a reddish marly horizon (about 1 m-thick), probably due to the presence of oxydized minerals, while thin reddish horizons were observed in the upper portion. In particular, in the uppermost portion of this lithofacies (36 m above the base of the Pietrasecca section) one of the thin reddish horizons, a few centimeters thick, shows a clear volcaniclastic nature because of the presence of fine-grained quartz, plagioclase, k-feldspar

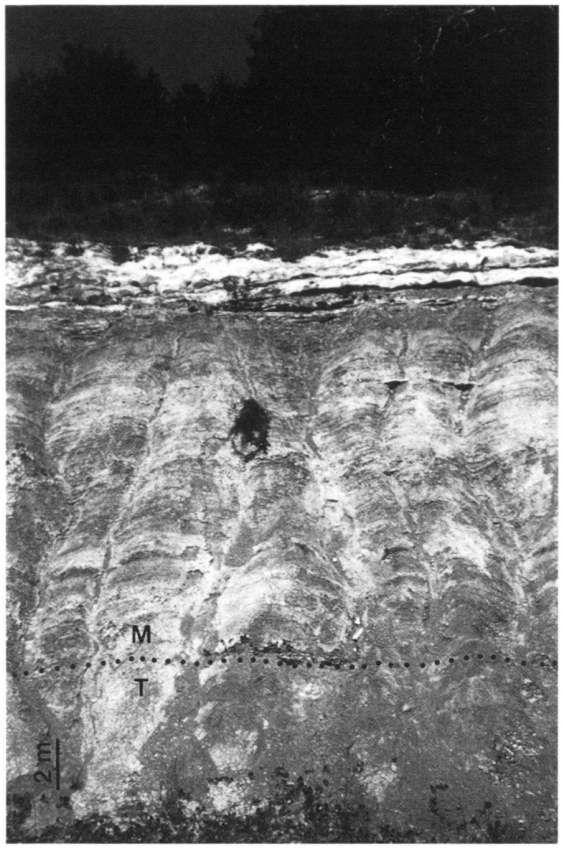

Fig. 4. Upper portion of the Pietrasecca section (about 30 out of 60 m total are shown). The picture shows the upper part of the *Marne a Orbulina* Fm. (bottom) and the lower part of the *Argilloso-arenacea* Fm. (top).

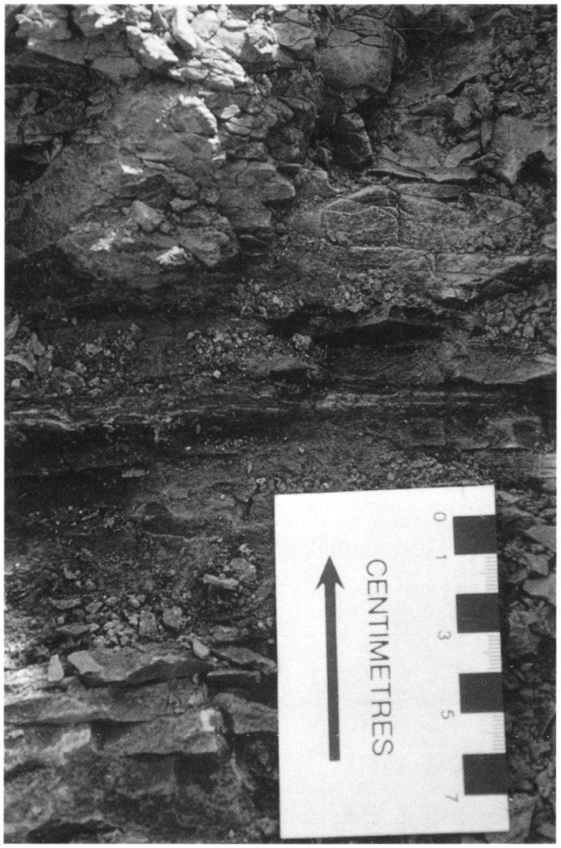

Fig. 5. Volcaniclastic level interbedded in the upper part of the *Marne a Orbulina* Fm., Pietrasecca section, marking the T/M boundary.

and biotite (Figs. 5 and 6). This portion of the section corresponds to the lower part of lithofacies 3 of Pampaloni et al. (1994).

Upsection, the *Argilloso-arenacea* Fm. starts with the appearance of turbiditic layers. The base of this formation is characterised by a pelitic-arenaceous siliciclastic unit with 3–4 cm-thick siltitic-arenaceous levels showing Tc-Td Bouma's sedimentary structures. This lithofacies is 11 m-thick and in the upper part it contains a channelised calciruditic deposit mainly made up of clasts deriving from the erosion of Meso-Cenozoic shallow-water limestones. The grain-flow character of this deposit together with the presence of turbiditic siliciclastic levels indicates that this lithofacies was deposited in a foredeep basin. In our opinion, the first gravity-flow recorded in the Pietrasecca section (*i.e.* the bottom of this lithofacies) marks a change in the sedimentary environment from an hemipelagic platform, related to a foreland flexure stage, to a foredeep basin. The pelitic-arenaceous association corresponds to the uppermost part of lithofacies 3 of Pampaloni et al. (1994).

An arenaceous-pelitic siliciclastic association is well recognisable at the top of this lithofacies in the Pietrasecca section (Fig. 3). This new lithofacies is characterised by the presence of thick arenaceous turbidites (1–6 m) which show Ta-Td Bouma's sedimentary structures, intercalated in a marly-clay pelagic deposit (*Argilloso-arenacea* Fm.; Cipollari et al. 1993).

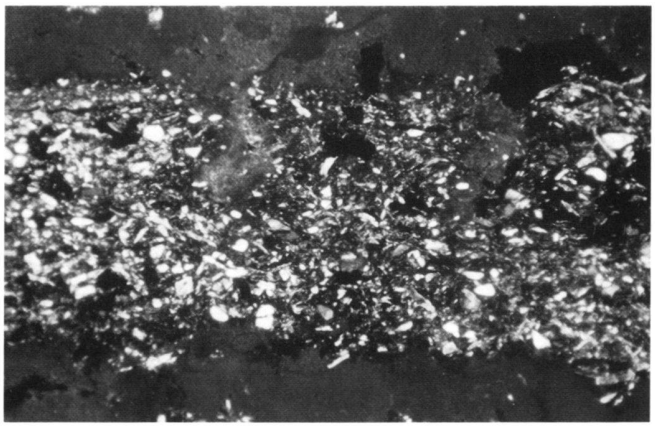

Fig. 6. Close up of the volcaniclastic level of Fig. 5 observed in thin section. Its andesitic affinity is suggested by the presence of labradoritic and andesinic plagioclase (grey spots). In the level are also present quartz (white spots), k-feldspar (grey spots) and biotite.

The Tufo Basso section

This section is located on the forelimb of the Pietrasecca-Tufo Basso anticline, a few kilometers to the NW of the Pietrasecca section. It is characterised by a 7 m-thick succession of Orbulina marls containing a reddish-marly horizon at the bottom. For its stratigraphic position and thickness, the latter can be correlated with the lowermost reddish-marly horizon observed in the Pietrasecca section.

Since the lower part of the Pietrasecca section does not offer good exposures for paleomagnetic sampling, the Tufo Basso section was investigated to extend the paleomagnetic study in depth.

Calcareous plankton biostratigraphy

Two different samples were collected from each stratigraphic level of the Pietrasecca section to perform the biostratigraphical analysis both of foraminifera and calcareous nannofossil assemblages.

Fortyfour samples, spaced of about 1 m, were collected from the top of the *Calcari a briozoi e litotamni* Fm. up to the lower part of the turbiditic deposits of the *Argilloso-arenacea* Fm., including the whole *Marne a Orbulina* Fm.

Calcareous nannofossils

Most of the samples from the lower part of the *Marne a Orbulina* Fm. are devoid of nannofossils. Due both to etching and overgrowth, the other samples collected from the same stratigraphic interval show very poorly preserved nannofossil assemblages. In this stratigraphic interval terrigenous dilution is also present.

In the middle and higher part of the *Marne a Orbulina* Fm. the calcareous nannofossils are more abundant and better preserved. On the contrary, the samples collected from the basal portion of the *Argilloso-arenacea* Fm. are devoid of nannofossils or characterised by very diluted and poorly preserved assemblages. The identification of the index species is also prevented by reworking, which is particularly strong in samples from the base and top of the Pietrasecca composite section.

A quantitative analysis of discoasterids was performed by counting a fixed number (100) of the most representative species. Furthermore, a qualitative analysis was conducted on forms belonging to the genus *Amaurolithus*, which are generally very rare.

The index species *Discoaster quinqueramus*, whose FO defines the base of CN 9 zone (upper Tortonian) (Okada & Bukry 1980) is present in the basal portion of the *Marne a Orbulina* Fm. In the studied section the presence of this species is very discontinuous. It was first observed in the sample PDD 8, about 7 m above the stratigraphic boundary between *Calcari a briozoi e litotamni* Fm. and *Marne a Orbulina* Fm. Since neither the lower samples nor those collected just above PDD 8 contain *D. quinqueramus*, we cannot recognise its FO. On the contrary, Pampaloni et al. (1994) using the occurrence of *Coccolithus miopelagicus* assign this portion of the section to the Serravallian, pointing out a sedimentation hiatus of about 2.5 Ma ten metres below the T/M boundary. However, the presence of five-rayed discoasters allows us to refer the basal portion of the Pietrasecca section at least to a Tortonian age.

The FO of the genus *Amaurolithus (A. primus)* was recognised in sample PDD 23, located about 35 m above the top of the *Calcari a briozoi e litotamni* Fm. Moreover, 3 m above the level in which this event occurs, in sample PDD 26, the FO of *A. delicatus* was recorded. This event was reported slightly after the FO of *A. primus* also by other authors both in Mediterranean and oceanic sediments (Flores & Sierro 1987; 1991; Rio et al. 1990; Flores et al 1992). This seems to be the best event among the calcareous nannofossils to approximate the Tortonian/Messinian boundary (Mazzei 1977; Salvatorini & Cita 1979; Flores et al. 1992).

The quantitative analysis of forms of the genus *Discoaster* pointed out some significant variations of the frequence of *D. variabilis* and of *D. pentaradiatus*. The first species shows a decrease of its abundance in an interval ranging between the FO of *A. primus* and the FO of *A. delicatus*. In the same stratigraphic interval the percentage of *D. pentaradiatus* increases and a trend of upward increase is observed starting from this point.

The other observed forms of *Discoaster (D. quinqueramus, D. bellus, D. brouweri, D. intercalaris, D. pseudovariabilis)* do not show any significant variation of their abundance throughout the section.

Finally, we observed several forms of placoliths not having a significant range but characterising the assemblage of all the samples: *Helicosphaera carteri, Pontosphaera sp., Sphenolithus abies, Reticulofenestra pseudoumbilicus, Calcidiscus leptoporus, C. macintyrei, Dictyococcites productus.*

Planktic foraminifera

The analysis of the foraminiferal assemblages of the Pietrasecca section allowed us to define the chronostratigraphic range of the sequence and to relate it to Iaccarino's zonal scheme (1985) for the Mediterranean area.

With regard to the "*menardii* form" globorotaliids, we referred to Tjalsma's classification (1971).

The basal portion of the Pietrasecca section (samples PDD 2–6) is characterised by a few specimens of *Neogloboquadrina acostaensis*, unkeeled globorotaliids (*Globorotalia* gr. *scitula*) and a very abundant, well-diversified benthic assemblage (*Anomalinoides* spp., *Uvigerina* spp., *Heterolepa dertonensis*).

From sample PDD 7 upward the benthic assemblages are considerably less abundant and some planktic bioevents are recognised at the top of the section.

In sample PDD 7 the FOs of *Globorotalia menardii* form 4 and *Globigerinoides obliquus extremus* are recorded; above 19 m (sample PDD 16) the FOs of *Globorotalia suterae* and *Globorotalia humerosa* follow, while FO of *Globorotalia menardii* form 5 is recognised in sample PDD 22 .

This part of the section is characterised by an abundant, but not well-preserved, planktic assemblage predominantly made up of *Neogloboquadrina acostaensis, Globorotalia* gr. *scitula, Globigerinoides obliquus extremus, Dentoglobigerina altispira, Globigerinoides sacculifer, Globigerina falconensis* and *Globorotalia menardii* form 4. Upward, immediately after the disappearance of *Globorotalia menardii* form 4, *Neogloboquadrina humerosa* and *Globorotalia menardii* form 5 are also present. In sample PDD 24 the genus *Globigerinoides* is particular abundant.

In this study, quantitative analyses have not been made because of the scarcity and very poor preservation of the foraminiferal faunas. However, a preliminary investigation on *Globorotalia menardii* forms 4 and 5 showed that *G. menardii* form 4 is present predominantly with sinistral specimens; this is in agreement with Sierro et al. 1993 (group I) and Glaçon et al. 1990 (event I). No evident preferential coiling variation has been recorded in *Globorotalia menardii* form 5, contrary to the dextral coiling direction reported by the previous authors (group II, Sierro et al. 1993; event II, Glaçon et al. 1990).

In sample PDD 26 the FO of *Globorotalia conomiozea* is recorded with sinistral morphotypes, followed by the FO of *Globorotalia mediterranea* (sample PDD 31).

In the upper part of the section (from sample PDD 26 up to the top), the foraminiferal fauna becomes scanty; the benthic assemblage, represented by *Bulimina echinata* and *Bolivina dentellata*, is reduced and completely absent from some levels (samples PDD 26 and PDD 29). The planktic assemblage consists of specimens with reduced size and, in some levels (samples PDD 26, PDD 29 and PDD 36), only small globigerinids were observed. The assemblage is predominantly represented by *Globorotalia conomiozea, Globigerina falconensis, Neogloboquadrina pachyderma, Turborotalita quinqueloba, Globorotalia saphoae, Globorotalia saheliana, Globigerinoides quadrilobatus* and *Globorotalia mediterranea.*

In conclusion, the foraminiferal analysis conducted in the Pietrasecca section allowed us to recognise some significant bioevents and to place the T/M boundary at the FO of *G. conomiozea.* The succession of bioevents at Pietrasecca (FO of *G. menardii* form 4, FO of *G. menardii* form 5 and FO of *G. conomiozea*) is well comparable with that recorded by other Mediterranean sections (Krijgsman et al. 1994).

$^{40}Ar/^{39}Ar$ dating

A plagioclase was carefully handpicked from the volcaniclastic level occurring at 36 meters from the bottom of the section, and its age estimated using the $^{40}Ar/^{39}Ar$ method. It was irradiated using Fish Canyon Tuff (FCT) biotite as an age monitor (27.55 Ma, Lanphere et al. 1990) and analysed following the procedure in use at the Istituto di Geocronologia e Geochimica Isotopica, CNR, Pisa (Laurenzi & Villa 1989; Cioni et al. 1993). Table 1 gives the analytical data, comprehensive of the total age (9.38 Ma), calculated from the sum of the radiogenic ^{40}Ar and ^{39}Ar of all steps. In Figure 7 the result obtained is shown as age spectrum (left scale, continuous line, displayed error 1σ), while the thick dashed line indicates the Ca/K ratio (right scale). Far from ideal, the spectrum is saddle shaped with the youngest step at 7.17 Ma. Two processes may be re-

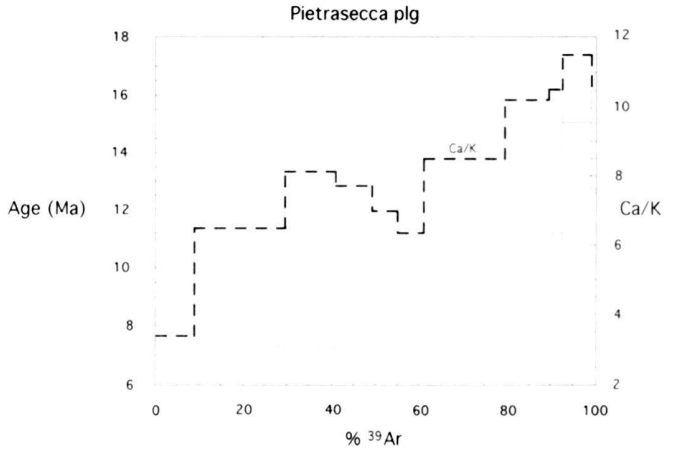

Fig. 7. Age spectrum of Pietrasecca plagioclase from sample PDD 26. The height of age boxes is related to the analytical error (1σ). The thick dashed line is indicative of the Ca/K ratio (see text for explanation).

Tab. 1. Analytical data relative to the $^{40}Ar/^{39}Ar$ step-heating experiment on plagioclase. Isotope concentrations are in ml/g, and are corrected for instrumental background, isotopic fractionation and ^{37}Ar decay only. Ages are corrected for all other sources of error.

PIETRASECCA PLAGIOCLASE J=4.196 E-4 w=146.03 mg

T(°C)	$^{40}Ar_{tot}$	^{39}Ar	^{38}Ar	^{37}Ar	^{36}Ar	Age (Ma)
700	2.576 E-07 ± 5	1.775 E-09 ± 7	1.65 E-10 ± 2	3.00 E-09 ± 2	7.79 E-10 ± 5	11.80 ± 0.60
830	7.469 E-08 ± 16	4.024 E-09 ± 13	7.63 E-11 ± 10	1.29 E-08 ± 1	1.27 E-10 ± 1	7.21 ± 0.06
900	3.048 E-08 ± 4	2.279 E-09 ± 6	3.53 E-11 ± 9	9.20 E-09 ± 4	3.27 E-11 ± 8	7.17 ± 0.08
960	2.669 E-08 ± 4	1.652 E-09 ± 5	2.80 E-11 ± 4	6.35 E-09 ± 3	3.69 E-11 ± 8	7.46 ± 0.11
1030	3.138 E-08 ± 6	1.203 E-09 ± 6	2.62 E-11 ± 10	4.19 E-09 ± 2	6.14 E-11 ± 11	8.53 ± 0.20
1100	4.278 E-08 ± 11	1.160 E-09 ± 4	3.25 E-11 ± 11	3.67 E-09 ± 2	9.62 E-11 ± 9	9.56 ± 0.18
1190	1.354 E-07 ± 2	3.601 E-09 ± 7	1.06 E-10 ± 1	1.53 E-08 ± 1	3.08 E-10 ± 2	9.56 ± 0.15
1280	6.956 E-08 ± 11	1.912 E-09 ± 4	5.49 E-11 ± 11	9.75 E-09 ± 5	1.52 E-10 ± 1	10.11 ± 0.13
1350	2.926 E-08 ± 6	6.839 E-10 ± 30	2.13 E-11 ± 4	3.58 E-09 ± 2	6.66 E-11 ± 8	10.91 ± 0.27
1400	9.498 E-08 ± 7	1.295 E-09 ± 3	5.99 E-11 ± 9	7.40 E-09 ± 4	2.35 E-10 ± 2	15.31 ± 0.25
1500	4.723 E-08 ± 11	1.424 E-10 ± 11	2.87 E-11 ± 5	7.51 E-10 ± 6	1.51 E-10 ± 1	14.43 ± 1.70
total age						9.38

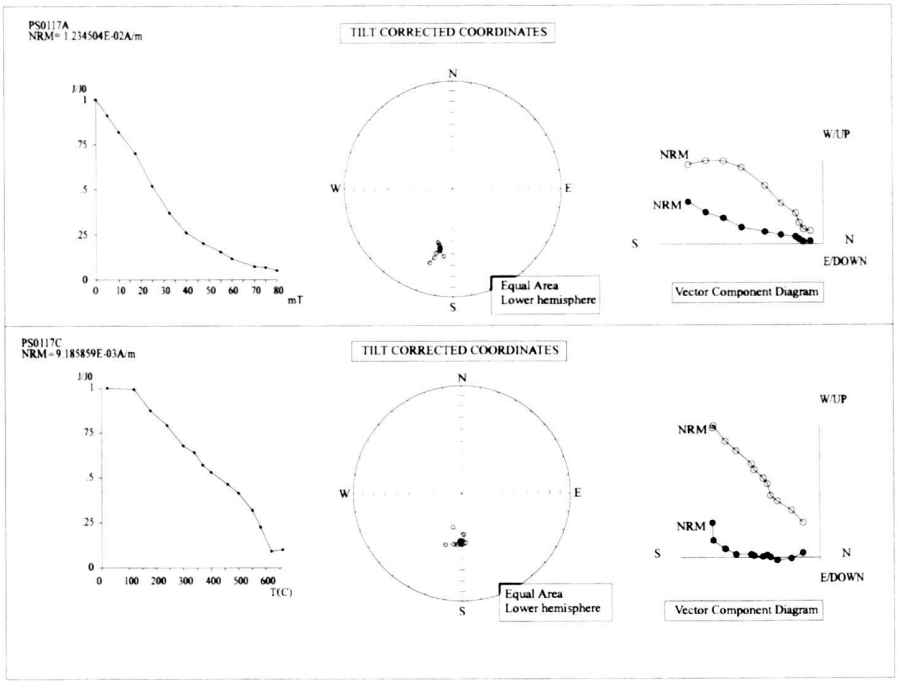

Fig. 8. Thermal and AF demagnetization diagrams in tilt corrected coordinates for two representative "sister" pilot specimens. Normalised intensity versus demagnetization field plots, equal area projections (open circles = upper hemisphere; full circles = lower hemisphere) and vector component diagrams (open circles = vertical projection; full circles = horizontal projection).

sponsible for this shape; 1) the presence of parentless ^{40}Ar in the mineral lattice at its formation, or 2) the presence of a mixed population of different ages. We cannot discriminate between the two hypotheses; we do know that two types of plagioclase are present in the sample, an andesinic one and a labradoritic one, but they may be coexistent and therefore are not necessarily representative of a mixed population. The Ca/K ratio generally tends to increase with the temperature, except from 30 to 60% of gas release, where there is a decrease. This is probably due to common zoning.

No clear age information is obtained from this sample, and we can only infer that the age is equal or younger than the age of the saddle bottom, which is 7.17 Ma. In samples disturbed like this, the total age is meaningless.

Magnetostratigraphy

Sampling and laboratory analyses

Only the upper part of the Pietrasecca section (30 m thick) was sampled for magnetostratigraphic analyses, due to bad outcrop conditions of the lower interval. In order to extend the palaeomagnetic investigation downward, we also sampled the Tufo Basso section (thickness 7 m), a few kilometers to the NW of the Pietrasecca section.

The palaeomagnetic sampling was carried out using a gasoline powered drill corer and orienting the cores in situ using a magnetic compass. Much effort was spent removing the weathered surface, in order to drill in sediments as fresh as possible. One hundred cores, 25 mm in diameter, were taken with an average spacing of about 30 cm. Laboratory measurements were carried out on at least one standard 22 mm high cylindrical specimen from each core. Magnetic remanences were measured using a JR-5 spinner magnetometer and the low-field magnetic susceptibility (k) was measured using a KLY-2 kappabridge.

Two sister pilot specimens were analyzed for some regularly spaced cores. For each couple of pilots, one was demagnetized by alternating field (AF) in steps of 2.5–10 mT up to 80–90 mT using a Molspin tumbler apparatus, the other was thermally demagnetized in 30 or 60°C steps from room temperature up to 660–680°C using a magnetically shielded electrical furnace. The pilot results showed that both demagnetization techniques isolated the same stable paleomagnetic component (Fig. 8). We used thermal demagnetization, in steps of 20–50°C, for all the remaining specimens. The low field magnetic susceptibility was monitored after each heating step, in order to detect possible thermally induced changes in the magnetic mineralogy.

Demagnetization results were examined using orthogonal vector diagrams (Zijderveld 1967), stereographic projections and intensity decay curves, and treated using principal component analysis (PCA) (Kirschvink 1980).

Rock magnetism analyses were performed on representative specimens to investigate the magnetic mineralogy and to check its homogeneity throughout the sections. We determined the:

- stepwise acquisition of an isothermal remanent magnetization (IRM), up to 1.6 Tesla (T);

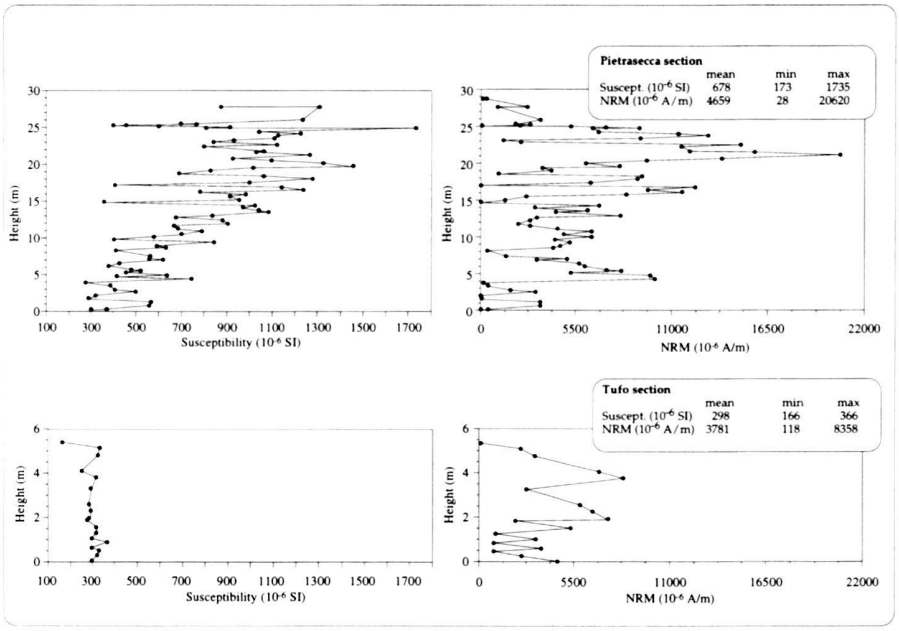

Fig. 9. Stratigraphic plots of the initial low-field susceptibility and NRM intensities in the Pietrasecca and Tufo Basso sections.

- remanence coercive force (Bcr), evaluated by back-field application to the saturation IRM;
- stepwise thermal demagnetization of a three-component IRM (Lowrie 1990). In this study, the applied fields were 1.6 T, 0.6 T and 0.12 T. The bulk susceptibility was monitored after each heating step;
- the ratio of saturation IRM to susceptibility (SIRM/k) and the ratio of the IRM in a backfield of 100 mT to the saturation IRM (SIRM) in a forward field of 1T (S-ratio) (Stober & Thompson 1979).

Results

Rock magnetism

In the Pietrasecca section the natural remanent magnetization (NRM) intensity and the low field magnetic susceptibility are in the range 28–20620 mA/m (mean value 4659 mA/m) and 173–1735 $\times 10^{-6}$ SI (mean value 678 $\times 10^{-6}$ SI), respectively. In the Tufo Basso section these values are slightly lower, 118 – 8358 mA/m (mean value 3781 mA/m) and 166 – 366 $\times 10^{-6}$ SI (mean value 298 $\times 10^{-6}$ SI), respectively. Both parameters show a marked cyclicity, that is particularly evident in the Pietrasecca section (Fig. 9). Moreover, the magnetic susceptibility follows an increasing trend in the upper part of the sequence, which is likely due to the intensification of the detrital inputs.

More than 90% of the saturation magnetization is generally reached in fields of 0.2–0.3 T and the coercivity of remanence is in the range of 28–45 mT. In the Pietrasecca section the SIRM/k ratio is in the range of 1.4–8.2 kA/m and the S-ratio is between –0.9 and –0.3. In the Tufo Basso section the same ratios range between 9.2 and 11.0 kA/m and between –0.7 and –0.8, respectively. This indicates that the magnetic mineralogy is dominated by low-coercivity minerals throughout both sections. The thermal demagnetization of a composite IRM confirms that a large portion of the remanence resides in the soft-coercivity fractions (≤ 0.12 T). The remanence intensities decrease in a quasi-linear fashion from room temperature to 580–610°C (Fig. 10). Only minor traces of hard coercivity minerals (hematite) were found in a few specimens. The abrupt increase in susceptibility at about 400°C suggests a thermally induced growth of new magnetic minerals.

In conclusion, rock magnetism analyses are consistent with magnetite being the main magnetic carrier. At some intervals cation deficent magnetite is suggested by Curie temperatures slightly in excess of 580°C (Heider & Dunlop 1986).

Palaeomagnetism

Thermal magnetic cleaning of the samples from the Pietrasecca composite section showed a rather constant behaviour throughout the section, with two components found in most of the specimens. Usually, after the removal of a low stability (viscous) component at 120°C, the demagnetization diagrams show stable and well defined characteristic remanent magnetization (ChRM), in most cases completely removed at temperatures ranging from 550 to 610°C. Further demagnetization at higher temperatures results in random directions. All the linear paths fitted to magnetization directions are characterised by maximum angular deviation (MAD) ≤ 10° (Fig. 11). In a few

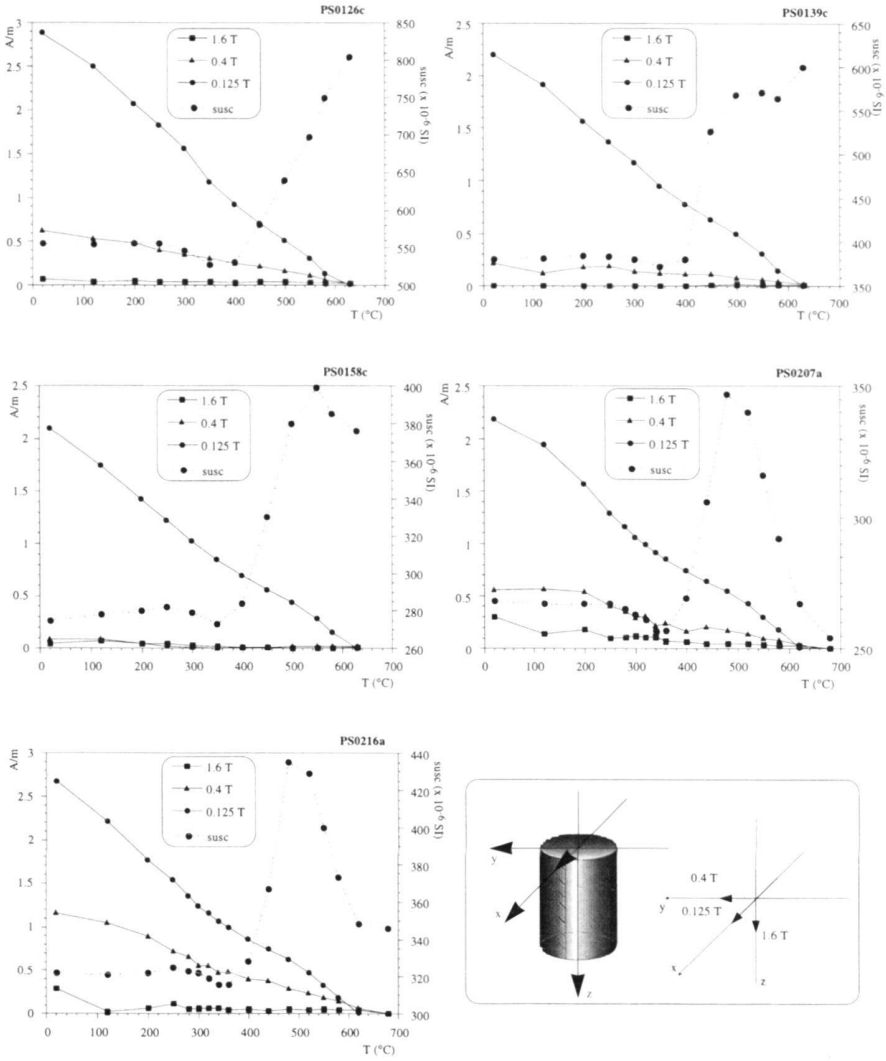

Fig. 10. Stepwise thermal demagnetization of a composite IRM (sequentially produced in fields of 1.6, 0.6 and 0.125 T, respectively) and bulk susceptibility changes during heating for five representative specimens.

specimens no stable end-point was reached during the demagnetization, due to the presence of two paleomagnetic components with largely overlapping blocking temperature spectra. For such specimens the best-fit remagnetization circles were calculated. Moreover, in six specimens collected from the Pietrasecca section and one from the Tufo Basso section the room temperature NRM shows such a low intensity (about 4×10^{-5} A/m) that paleomagnetic data are uncertain and cannot be interpreted. The magnetostratigraphic data for the two sections are shown in Figure 12.

In the Pietrasecca section the reliable ChRM directions, after tectonic correction (atc), group in two antipodal clusters defined by Fisher's statistics (1953) as declination D = 340.4°, inclination I = 40.8° (α_{95} = 8.6°) for the normal polarity and D = 171.1°, I = –45.4° (α_{95} = 4.8°) for the reverse (Tab. 2). The two groups show a positive reversal test of the type R_B, according to the classification by McFadden & McElhinny (1990) (Tab. 3).

In the Tufo basso section, the reliable ChRMs (atc) are clustered in two antipodal groups defined by D = 343.7°, I = 50.6° (α_{95} = 10.0°) for the normal polarity and D = 174.2°, I = –53.6° (α_{95} = 8.9°) for the reverse (Tab. 2), with a positive reversal test of the type R_C (Tab. 3).

The westward declinations indicate about 15° of counterclockwise rotation after the Messinian for the Pietrasecca anticline, as already pointed out by Mattei et al. (1995).

The mean inclination value for both the normal and reverse polarity samples is slightly lower than the value expected (62°) at the site latitude (43° N), assuming a geocentric axial dipolar field. The inclination shallowing is probably related to compaction and is enhanced in the upper part of the Pietrasecca section due to the increasing input of the clay fraction.

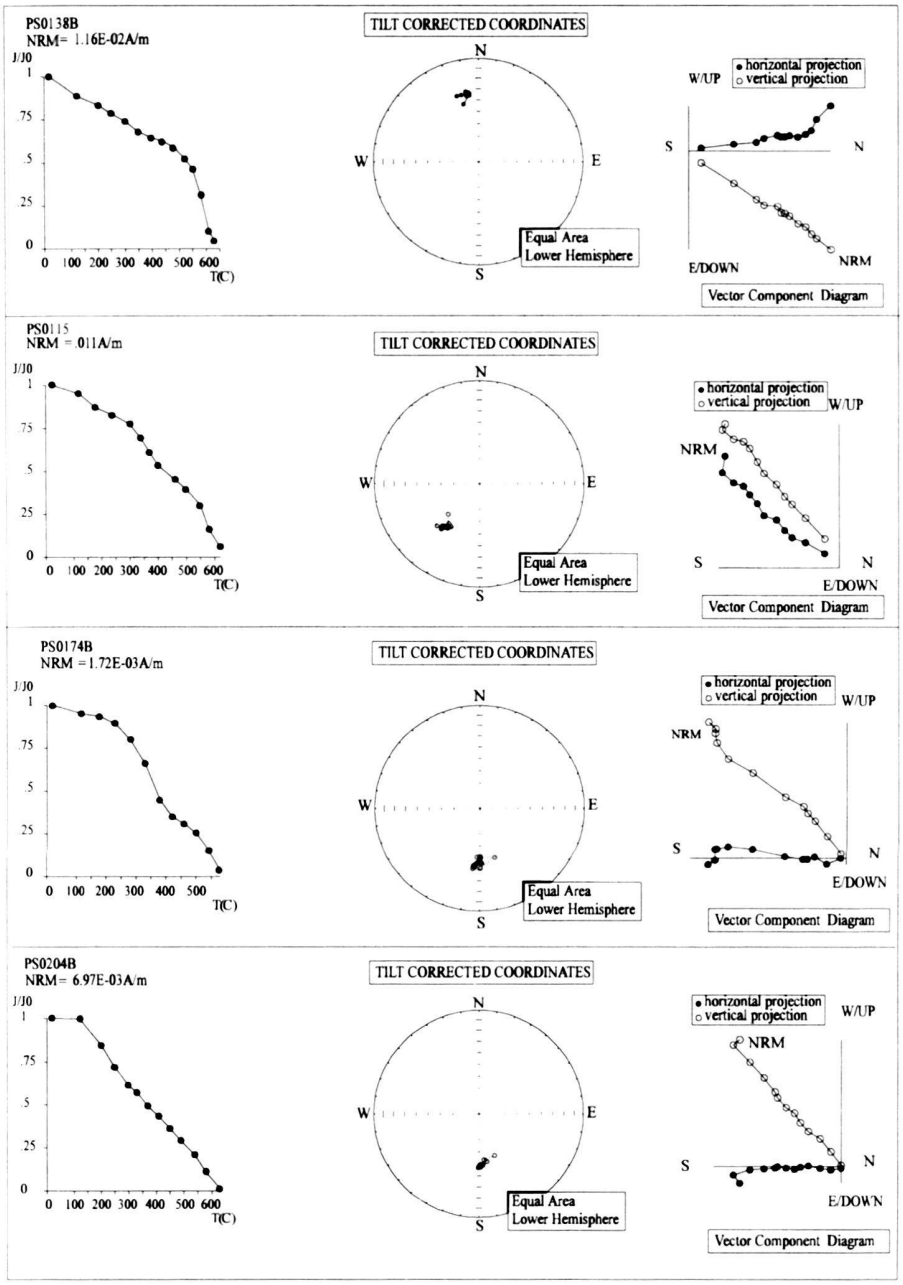

Fig. 11. Thermal demagnetization diagrams in tilt corrected coordinates for four representative specimens. Normalised intensity versus demagnetization field plots, equal area projections (open circles = upper hemisphere; full circles = lower hemisphere) and vector component diagrams (open circles = vertical projection; full circles = horizontal projection).

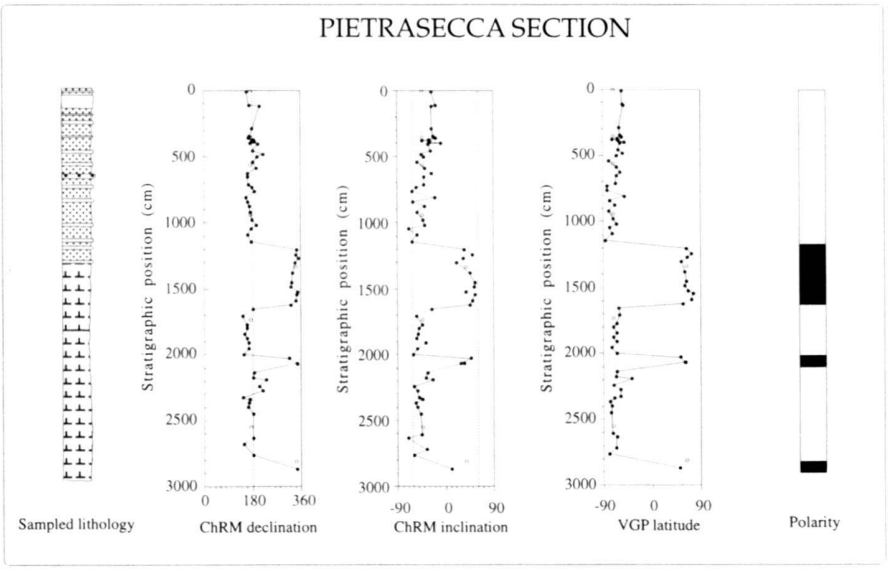

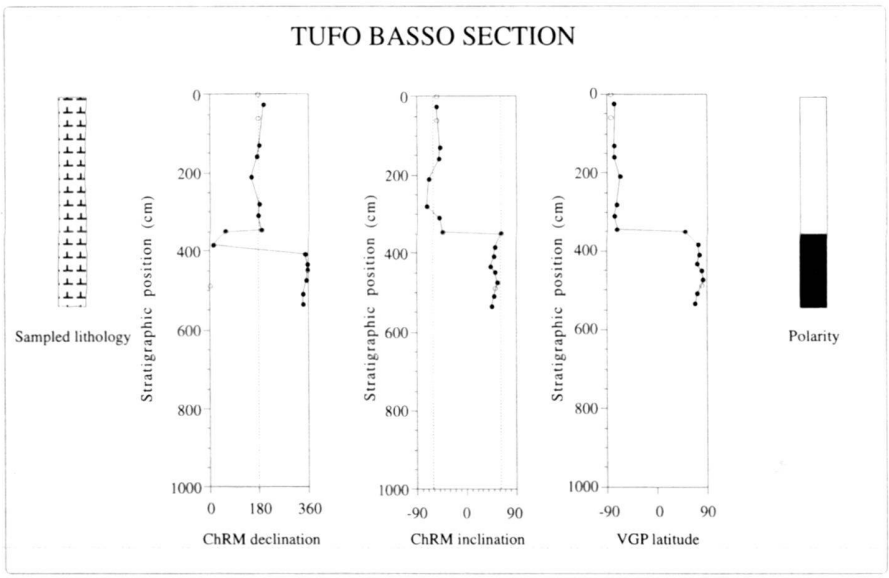

Fig. 12. Lithology, declinations, inclinations, VGP latitudes and polarity zonation of magnetostratigraphic specimens from the Pietrasecca (a) and Tufo Basso (b) sections. Paleomagnetic data: dots represent specimens with reliable characteristic remanent magnetizations (ChRM) isolated during the demagnetization treatment, open circles indicate specimens for which the ChRM cannot be directly isolated during the demagnetization, since they describe "remagnetization circles" not reaching a stable end-point. For these latter specimens the plotted mean value has been computed from the combined analyses of remagnetization circles and stable end-points (McFadden & McElhinny 1988) throughout each section.

Tab. 2 - Summary of palaeomagnetic data

Pietrasecca *(bedding 48, 55)*

Polarity	*N*	*Dec (btc)*	*Inc (btc)*	*Dec (atc)*	*Inc (atc)*	*k*	α_{95}
Normal	12 (14)	290.2	37.7	340.4	40.8	26.7	8.6
Reversed	42 (52)	106.3	-46.3	171.1	-45.4	22.4	4.8
Total	54 (66)	287.3	44.4	348.6	44.4	22.5	4.2

Tufo Basso *(bedding 36, 52 - by anisotropy)*

Polarity	*N*	*Dec (btc)*	*Inc (btc)*	*Dec (atc)*	*Inc (atc)*	*k*	α_{95}
Normal	5 (8)	269.6	51.4	343.7	50.6	59.6	10.0
Reversed	7 (7)	83.5	-57.6	174.2	-53.6	47.4	8.9
Total	12 (15)	266.3	55.0	349.6	52.5	50.9	6.1

N = number of samples;
atc = after tectonic correction;
btc = before tectonic correction;
k, α_{95} = precision parameter and half-angle of the 95% confidence cone about the mean direction.

Tab. 3 - Results of reversal test (McFadden and McElhinny, 1990)

Pietrasecca

k_n/k_r	γ	γ_c	*class*
1.2	9.0	9.7	R_B

Tufo Basso

k_n/k_r	γ	γ_c	*class*
1.2	7.1	12.8	R_C

γ - angle between the two means;
γ_c - critical angle;
k_n, k_r - precision parameters (Fisher, 1953) related to the normal and reverse polarity clusters.

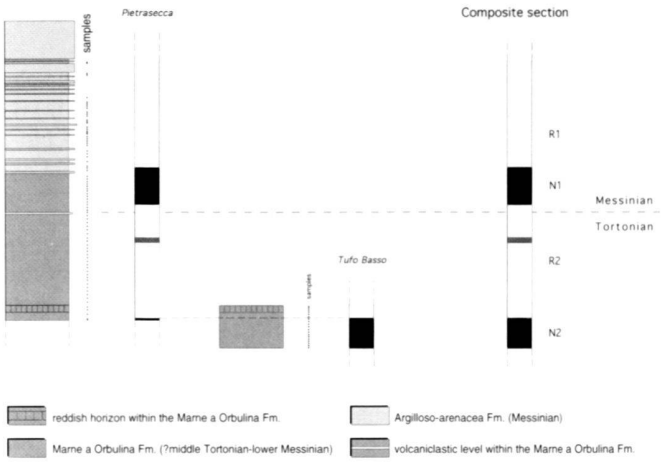

Fig. 13. The Pietrasecca composite section reconstructed on the basis of lithology and magnetostratigraphy from the Pietrasecca and Tufo Basso sections.

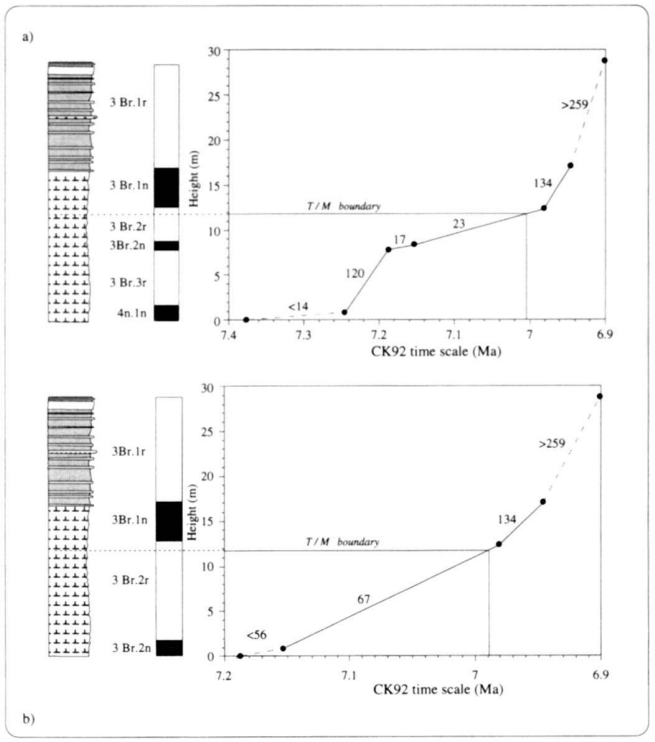

Fig. 14. Age-height relationship and sedimentation rates based on correlating the obtained polarity stratigraphy with the CK92 GPTS (numbers on curves represent the sedimentation rates in m/Ma). In this magnetostratigraphic solution the T/M boundary is at the top of C3Br.2r considering the FO of *A. primus* as an isochronous event. In (a) solution the short normal event observed within the reverse magnetozone R2 has been correlated with the C3Br.2n, whereas in (b) the same event has been considered as a short event within the C3Br.2r (Florindo 1996).

Correlation to the Global Polarity Time Scale (GPTS)

The stratigraphic plots of the ChRM directions and the virtual geomagnetic poles (VGPs) latitude exhibit a clear pattern of magnetozones, labelled from R1–N1 to R2–N2 (Fig. 13). Within the R2 reverse polarity zone, an extra short normal polarity interval was identified (Florindo 1996).

The FO of *G. conomiozea*, which defines the T/M boundary, was found in the R2 reverse magnetozone, in correspondence with the volcaniclastic level which yielded the sample used for $^{40}Ar/^{39}Ar$ chronological information (≤ 7.17 Ma). Within the same interval, the FO of *A. primus* and the co-occurrence of *A. delicatus* and *G. conomiozea* were also recognised.

Comparing the data obtained from the tropical Indian Ocean with data from the equatorial Pacific, Raffi et al. (1995) concluded that the FO event of *A. primus* is isochronous in the two areas, where this bioevent occurs within C3Br. In particular, at ODP Sites 710 (tropical Indian Ocean), 844 and 845 (equatorial Pacific Ocean) *A. primus* appears within C3Br.2r (Raffi 1992; Raffi et al. 1995). In the Atlantic Ocean (DSDP 608) Gartner (1992) indicates that the FO of *A. primus* is probably slightly diachronous with respect to the Indian and the Pacific Oceans, even if in correspondence of this bioevent at DSDP Site 608 the correlation of the magnetostratigraphic record to the GPTS is not sufficiently accurate. In particular, the C3B chron seems to be completely missing. For this reason, we think that the diachrony of the FO of *A. primus* between Indo-Pacific low-latitude areas and the north Atlantic Ocean, as suggested by Gartner (1992), is not supported by magnetostratigraphic data.

Assuming the FO of *A. primus* as globally isochronous and taking into account the results from ODP Legs 115, 130 and 138 (equatorial Indian and Pacific oceans), showing the FO of *A. primus* within C3Br.2r (Raffi 1992; Raffi et al. 1995), we correlate the polarity sequences recognised in the Pietrasecca composite section with the CK92 (Fig. 14). The proposed correlation is supported by the estimated sedimentation rates, based on the correlation of different magnetostratigraphic solutions with the geomagnetic reference scales. The best-fit among lithology, magnetostratigraphy and sedimentation rates is shown in Figure 14b. In the suggested calibration (Fig. 14b) the increases in sedimentation rate are closely connected with lithological variations recorded in the Pietrasecca section. In particular, the increase in sedimentation rate observed just above the T/M boundary is due to the thin siliciclastic turbiditic levels which characterise the basal portion of the Argilloso-arenacea Fm. (pelitic-arenaceous association). The first siliciclastic input occurs in the upper part of C3Br.1n. A further increase in sedimentation rate was found within C3Br.1r with the onset of the arenaceous-pelitic sedimentation.

We therefore suggest to correlate the R2 reversed magnetozone with the C3Br.2r subchron of CK92, containing the T/M boundary in its upper part. The short normal zone cannot

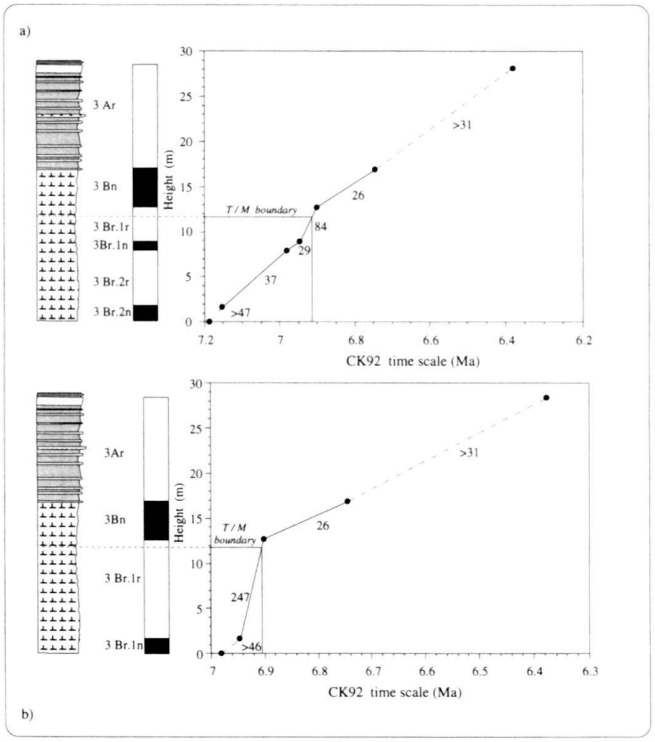

Fig. 15. Age-height relationship and sedimentation rates based on correlating the obtained polarity stratigraphy with the CK92 GPTS (numbers on curves represent the sedimentation rates in m/Ma). In this magnetostratigraphic solution the T/M boundary is at the top of C3Br.1r as suggested by Krijgsman et al. (1994). In (a) solution the short normal event observed within the reverse magnetozone R2 has been correlated with the C3Br.1n, whereas in (b) the same event has been considered as a short event within the C3Br.1r.

be correlated to any chron in CK92 and has been interpreted as a previously unrecognised event, within the C3Br.2r (Florindo 1996).

A different correlation to the GPTS has been suggested by Krijgsman et al. (1994; 1995). These authors define the T/M boundary using the First Regular Occurrence of *G. conomiozea* group (Krijgsman et al. 1995), which places this boundary in subchron C3Br.1r. Taking into account this different magnetostratigraphic solution, however, results in unrealistic changes in sedimentation rate (Fig. 15). In fact, the sedimentation rates calculated using the correlation suggested by Krijgsman et al. (1994; 1995) are in disagreement with the lithological variations observed in the Pietrasecca section.

Conclusions

According to biostratigraphy, magnetostratigraphy and sedimentation rates the T/M boundary in the Pietrasecca section falls in C3Br.2r (Fig. 16) with an age of 7.0 Ma according to the GPTS of Cande & Kent (1992) (CK92). On the other hand, the modified GPTS of Baksi (1993) provides for this boundary an age of 7.1 Ma, whereas 7.18 Ma is the age yielded by the GPTS of Cande & Kent (1995) (CK95).

The $^{40}Ar/^{39}Ar$ dating on plagioclase collected from the volcaniclastic level which marks the T/M boundary ($\leq$ 7.17 Ma) is in good agreement with the $^{40}Ar/^{39}Ar$ data provided by a biotite sample at the FAD of *G. conomiozea* in the Monte del Casino section (7.15 $\pm$ 0.04 Ma, Laurenzi et al., in press).

Acknowledgements

This study was carried out within the preliminary study for the acquisition of the CROP 11 seismic line (resp. M. Parotto), with financial support provided by MURST 40% (resp. A. Praturlon) and by the Istituto Nazionale di Geofisica. We wish to acknowledge H. Luterbacher and I. Premoli-Silva for their helpful reviews of the manuscript.

REFERENCES

Agostini, S. 1993: Carta geologica, scala 1:10.000. In: L'area carsica di Pietrasecca (Carsoli, Abruzzo). (Ed. by Burri, E). Mem. Ist. ital. Speleol., serie II, 5.

Aubouin, J., Debelmas, J. & Latreille, M. 1980: Les chaines alpines issues de la Téthys: introduction générale. Mem. Bur. Rech. Geol. Min. 115, 712.

Baksi, A.K. 1993: A geomagnetic polarity scale for the period 0–17 Ma, based on $^{40}Ar/^{39}Ar$ plateau ages for selected field reversals. Geophys. Res. Letters 20 (15), 1607–1610.

Benson, R.H. & Rakic-El Bied, K. 1991: Biodynamics, saline giants and Late Miocene catastrophism. Carbonates Evaporites 6, 127–168.

Berggren, W.A., Kent, D.V., Flynn, J.J. & Van Couvering, J.A. 1985: Cenozoic geochronology. Geol. Soc. Am. Bull. 96, 1407–1418.

Blow, H.M. 1969: Late Middle Eocene to Recent planktonic foraminiferal biostratigraphy. In: Proceedings of the First International Conference on Planktonic Microfossils (Ed. by Brönnimann, R. & Renz, H.H.). Leiden: E.J. Brill 1, 199–421.

Boccaletti, M. & Guazzone, G. 1972: Gli archi appenninici, il mare Ligure ed il Tirreno nel quadro della tettonica dei bacini marginali di retroarco. Mem. Soc. Geol. ital. 11, 201–216.

Boccaletti, M., Elter, P. & Guazzone, G. 1971: Plate tectonics model for the development of the Western Alps and Northern Apennines. Nature 234, 108–111.

Boccaletti, M., Coli, M., Decandia, F., Giannini, E. & Lazzarotto, A. 1980: Evoluzione dell'Appennino settentrionale secondo un nuovo modello strutturale. Mem. Soc. Geol. ital. 21, 359–374.

Cande, S.C. & Kent, D.V. 1992: A new Geomagnetic Polarity Time Scale for the Late Cretaceous and Cenozoic. J. Geophys. Res. 97, 12917–13951.

– 1995: Revised calibration of the geomagnetic polarity timescale for the Late Cretaceous and Cenozoic. J. Geophys. Res. 100, 6093–6095.

Channel, J.E.T., Torii, M. & Hawthorne, T. 1990: Magnetostratigraphy of sediments recovered at Sites 650, 651, 652 and 654 (Leg 107, Thyrrhenian Sea). Proc. ODP, Sci. Results 107, 335–346.

Cioni, R., Laurenzi, M.A., Sbrana, A. & Villa, I.M. 1993: $^{40}Ar/^{39}Ar$ chronostratigraphy of the initial activity in the Sabatini volcanic complex (Italy). Boll. Soc. Geol. ital. 112, 251–263.

Cipollari, P. & Cosentino, D. 1996: Miocene tectono-sedimentary events and geodynamic evolution of the central Apennines (Italy). Notes et Mém. Serv. Géol. Maroc, in press.

Cipollari, P., Cosentino, D. & Perilli, N. 1993: Analisi biostratigrafica dei depositi terrigeni a ridosso della linea Olevano-Antrodoco. Geologica Romana 29, 495–513.

Cipollari, P., Cosentino, D., Esu, D., Girotti, O., Gliozzi, E. & Praturlon, A. 1995: Central Apennines (Italy) accretionary wedge: recognition of lacustrine environment in a late Messinian thrust-top basin. Meeting of the IGCP-Project 324 on "Recent and ancient lacustrine systems in convergent margins" Antofagasta-Iquique-Calama-San Pedro de Atacama, Chile November, 12–18 1995, abstract, 34–35.

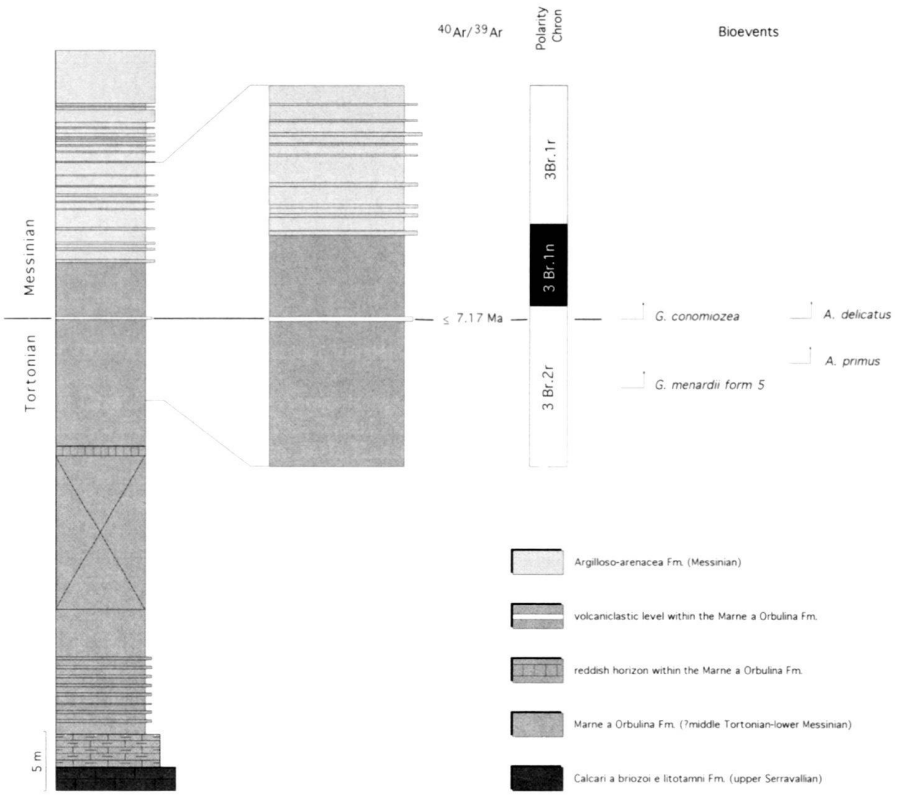

Fig. 16. Calibration of the Tortonian/Messinian boundary in the Pietrasecca section. The estimated age and the correlation with the CK92 GPTS are shown.

COLALONGO, M.L., DI GRANDE, A., D'ONOFRIO, S., GIANELLI, L., IACCARINO, S., MAZZEI, R., POPPI BRIGATTI, M.F., ROMEO, M., ROSSI, A. & SALVATORINI, G. 1979: A proposal for the Tortonian-Messinian boundary. Ann. Géol. Pays Hellén. 1, 285–294.

COMPAGNONI, B., GALLUZZO, F., PAMPALONI, M.L., PICHEZZI, R.M., RAFFI, I., ROSSI, M. & SANTANTONIO, M. 1992: Dati sulla lito-biostratigrafia delle successioni terrigene nell'area tra i Monti Simbruini e i Monti Carseolani (Appennino centrale). Studi Geol. Camerti vol. spec. 1991/2, 173–180.

CUNNINGHAM, K.J., FARR, M.R. & RAKIC-EL BIED, K. 1994: Magnetostratigraphic dating of an Upper Miocene shallow-marine and continental sedimentary succession in northeastern Morocco. Earth Planet. Sci. Lett. 127, 77–93.

FISHER, R.A. 1953: Dispersion on a sphere. Proc. r. Soc. London A217, 295–305.

FLORES, J.A. & SIERRO, F.J. 1987: Calcareous plankton in the Tortonian/Messinian transition series of the northwestern edge of the Guadalquivir basin. Abh. Geol. Bundesanst. 39, 67–84.

– 1991: Análisis factorial (modo Q) de la nanoflora calcárea del Mioceno superior en el sondeo ODP 654 (Tirreno, Mediterráneo occidental). Rev. Española Paleontologia 6, 50–58.

FLORES, J.A., SIERRO, F.J. & GLAÇON, G. 1992: Calcareous plankton analysis in the pre-evaporitic sediments of the Site 654 (Tyrrhenian Sea, western Mediterranean). Micropaleontology 38, 279–288.

FLORINDO, F. 1996: Record of a previously unidentified short geomagnetic event from an Upper Miocene sedimentary sequence, and preferred path of the transitional VGPs. Geophys. J. Int. 126, F1–F5.

GARTNER, S. 1992: Miocene nannofossil chronology in the North Atlantic, DSDP Site 608. Mar. Micropaleontol. 18, 307–331.

GLAÇON, G., VERGNAUD GRAZZINI, C., IACCARINO, S., REHAULT, J.P., RANDRIANASOLO, A., SIERRO, F.J., WEAVER, P., CHANNELL, J., TORII, M. & HAWTHORNE, T. 1990: Planktonic foraminiferal events and stable isotope record in the Upper Miocene of the Tyrrhenian Sea, ODP Site 654, Leg 107. Proc. ODP, Sci. Results 107, 415–427.

HEIDER, F. & DUNLOP, D.J. 1986: Two types of chemical remanent magnetization during oxidation of magnetite. Phys. Earth Planet. Inter. 46, 24–45.

HILGEN, F.J., KRIJGSMAN, W., LANGEREIS, C.G., LOURENS, L.J., SANTARELLI, A. & ZACHARIASSE, W.J. 1995: An astronomical (polarity) time scale for the Late Miocene. Earth Planet. Sci. Lett. 136, 495–510.

HODELL, D.A., BENSON, R.H., KENT, D.V., BOERSMA, A. & RAKIC-EL BIED, K. 1994: Magnetostratigraphic, biostratigraphic, and stable isotope stratigraphy of an Upper Miocene drill core from the Salé Briqueterie (northwest Morocco): A high-resolution chronology for the Messinian stage. Paleoceanography 9, 835–855.

IACCARINO, S. 1985: Mediterranean Miocene and Pliocene planktic foraminifera. In: Plankton Stratigraphy (Ed. by BOLLI, H.M., SAUNDERS, J.B. & PERCH-NIELSEN, K.) Cambridge (Cambridge Univ. Press), 283–314.

KRIJGSMAN, W., HILGEN, F.J., LANGEREIS, C.G. & ZACHARIASSE, W.J. 1994: The age of the Tortonian/Messinian boundary. Earth Planet. Sci. Lett. 121, 533–547.

KRIJGSMAN, W., HILGEN, F.J., LANGEREIS, C.G., SANTARELLI, A. & ZACHARIASSE, W.J. 1995: Late Miocene magnetostratigraphy, biostratigraphy and cyclostratigraphy in the Mediterranean. Earth Planet. Sci. Lett. 136, 475–494.

KIRSCHVINK, J.L. 1980: The least-squares line and plane and the analysis of palaeomagnetic data. Geophys. J. R. Astron. Soc. 62, 699–718.

LANGEREIS, C.G. 1984: Late Miocene magnetostratigraphy in the Mediterranean. Ph.D. Thesis, Univ. Utrecht, Geol. Ultraiectina 34.

LANGEREIS, C.G. & DEKKERS, M.J. 1992: Paleomagnetism and rock magnetism of the Tortonian-Messinian boundary stratotype at Falconara, Sicily. Phys. Earth Planet. Inter. 71, 100–111.

LANGEREIS, C.G., ZACHARIASSE, W.J. & ZIJDERVELD, J.D.A. 1984: Late Miocene Magnetobiostratigraphy of Crete. Mar. Micropalaeontol. 8, 261–281.

LANPHERE, M.A., SAWYER, D.A. & FLECK, R.J. 1990: High-resolution $^{40}Ar/^{39}Ar$ geochronology of Tertiary volcanic rocks, Western U.S.A. Geol. Soc. Australia Abs. 27, 57.

LAURENZI, M.A. & VILLA, I.M. 1989: $^{40}Ar/^{39}Ar$ chronostratigraphy of Vico ignimbrites. Per. Mineral. 56, 285–295.

LAURENZI, M.A., TATEO, F., VILLA, I.M. & VAI, G.B. in press: New radiometric datings bracketing the Tortonian/Messinian boundary in the Romagna potential stratotype sections (Northern Apennines). In: Miocene Integrated Stratigraphy (Ed. by MONTANARI, A., ODIN, G.S. & COCCIONI, R). Elsevier, Amsterdam, in press.

LOWRIE, W. 1990: Identification of ferromagnetic minerals in a rock by coercivity and unblocking temperature properties. Geophys. Res. Lett. 17, 159–162.

MANTOVANI, E., BABUCCI, D. & FARSI, F. 1985: Tertiary evolution of the Mediterranean region: major outstanding problems. Boll. Geofis. Teor. Appl. 105, 67–90.

MATTEI, M., FUNICIELLO, R. & KISSEL, C. 1995: Paleomagnetic and structural evidence for Neogene block rotations in the Central Apennines, Italy. J. Geophys. Research 100 (B9), 17,863–17,883.

MAZZEI, R. 1977: Biostratigraphy of the Rio Mazzapiedi-Castellania Section (type section of the Tortonian) based on calcareous nannoplankton. Atti Soc. Tosc. Sci. Nat., Mem. 84(a), 15–24.

MCFADDEN, P.L. & MCELHINNY, M.W. 1988: The combined analysis of remagnetization circles and direct observations in paleomagnetism. Earth Planet. Sci. Lett. 87, 161–172.

– 1990: Classification of reversal test in paleomagnetism. Geophys. J. Int. 103, 725–729.

MOREAU, M.G., FEINBERG, H. & POZZI, J.P. 1985: Magnetobiostratigraphy of a Late Miocene section from the Moroccan Atlantic margin. Earth Planet. Sci. Lett. 76, 167–175.

NEGRI, A. & VIGLIOTTI, L. in press: Calcareous nannofossil biostratigraphy and paleomagnetism of the Monte Tondo and Monte del Casino sections (Romagna Apennine, Italy). In: Miocene Integrated Stratigraphy (Ed. by MONTANARI, A., ODIN, G.S. & COCCIONI, R). Elsevier, Amsterdam, in press.

OKADA, H. & BUKRY, D. 1980: Supplementary modification and introduction of code numbers to the low-latitude coccolith biostratigraphic zonation (Bukry, 1973; 1975). Mar. Micropal. 5(3), 5–321.

PAMPALONI, M.L., PICHEZZI, R.M., RAFFI, I. & ROSSI, M. 1994: Calcareous plankton-biostratigraphy of the marne a *Orbulina* unit (Miocene, central Italy). G. Geologia 56/1, 139–153.

PAROTTO, M. & PRATURLON, A. 1975: Geological summary of the Central Apennines. Quad. Ric. Scient. 90, 257–311.

PATACCA, E., SCANDONE, P., BELLATALLA, M., PERILLI, N. & SANTINI, U. 1992: La zona di giunzione tra l'arco appenninico settentrionale e l'arco appenninico meridionale nell'Abruzzo e nel Molise. Studi Geol. Camerti vol. spec. 1991/2, 417–441.

RAFFI, I. 1992: Nannofossil biochronology of Middle Miocene to lowermost Pliocene in low-latitude environment: results from ODP leg 138 (Eastern Equatorial Pacific). I.U.G.S-S.O.G. Miocene Columbus Project, Ancona, 11–14, November, 1992. Abs., 92.

RAFFI, I., RIO, D., D'ATRI, A., FORNACIARI, E. & ROCCHETTI, S. 1995: Quantitative distribution patterns and biomagnetostratigraphy of Middle and Late Miocene calcareous nannofossils from equatorial Indian and Pacific Oceans (Leg 115, 130 and 138). Proc. ODP Sci. Results 138, 479–502.

RIO, D., FORNACIARI, E. & RAFFI, I. 1990: Late Oligocene through early Pleistocene calcareous nannofossils from western equatorial Indian Ocean (Leg 115). Proc. ODP Sci. Results 115, 175–235.

SALVATORINI, G. & CITA, M.B. 1979: Miocene foraminiferal stratigraphy, DSDP Site 397 (Cape Bojador, North Atlantic). Init. Rep. DSDP 47(1), 317–373.

SCANDONE, P. 1979: Origin of the Tyrrhenian sea and Calabrian arc. Boll. Soc. Geol. ital. 98, 27–34.

SHACKLETON, N.J., CROWHURST, S., HAGELBERG, T., PISIAS, N.G. & SCHNEIDER, D.A. 1995: A new late Neogene time scale: application to Leg 138 sites. In: Proc. ODP,. Sci. Results 138, 73–101.

SIERRO, F.J. 1985: The replacement of the "Globorotalia miotumida" group: An aid to recognizing the Tortonian/Messinian boundary in the Mediterranean and adjacent Atlantic. Mar. Micropaleontol. 9, 525–535.

SIERRO, F.J., FLORES, J.A., CIVIS, J., GONZÁLEZ DELGADO, J.A. & FRANCÉS, G. 1993: Late Miocene globorotaliid event-stratigraphy and biogeography in the NE-Atlantic and Mediterranean. Mar. Micropaleontol. 21, 143–168.

STOBER, J.C. & THOMPSON, R. 1979: Paleomagnetic secular variations studies of Finnish lake sediments and the carriers of remanence. Earth Planet. Sci. Lett. 37, 139–149.

TJALSMA, R.C. 1971: Stratigraphy and Foraminifera of the Neogene of the Eastern Guadalquivir Basin (Southern Spain). Utrecht Micropal. Bull. 4, 1–161.

VAI, G.B. in press: Cyclostratigraphic estimate of the Messinian Stage duration. In: Miocene Integrated Stratigraphy (Ed. by MONTANARI, A., ODIN, G.S. & COCCIONI, R.). Elsevier, Amsterdam, in press.

VAI, G.B., VILLA, I.M. & COLALONGO, M.L. 1993: First direct radiometric dating of the Tortonian/Messinian boundary. C. R. Acad. Sci. Paris 316, 1407–1414.

ZIJDERVELD, J.D.A. 1967: A.C. demagnetization of rocks: analysis of results. In: Methods in Paleomagnetism (Ed. by COLLINSON, D.W.). Elsevier, New York, 254–286.

Manuscript received August 5, 1996
Revision accepted March 4, 1997